Contents lists available at SciOpen

Food Science and Human Wellness

journal homepage: https://www.sciopen.com/journal/2097-0765

China Food Publishing Co.

Interactions between selenium-containing peptide Ser-Phe-Gln-SeM and intestinal microbiota: implications for antioxidant mechanism and host metabolism

Xing Zhang[a], Yucheng Xiang[a], Tao Hou[b], Chenyang Lu[c,*], Shaohua Huang[a,*]

[a] Institute of Drug Discovery and Technology, Ningbo University, Ningbo 315211, China
[b] College of Food Science and Technology, Huazhong Agricultural University, Wuhan 430070, China
[c] School of Marine Science, Ningbo University, Ningbo 315211, China

ARTICLE INFO

Article history:
Received 14 October 2024
Received in revised form 25 November 2024
Accepted 17 December 2024

Keywords:
Selenium-containing peptides
Antioxidant mechanism
Intestinal microbiota
Host interaction

ABSTRACT

The antioxidant activity of selenium-containing soybean peptides (SePPs) has been previously demonstrated, despite their limited absorption in the small intestine. This study investigates the antioxidant mechanism of a selenium-containing tetrapeptide, Ser-Phe-Gln-SeM (SFQSeM), identified from SePPs, with particular emphasis on its interaction with the intestinal microbiota and its role in modulating host antioxidant defenses. The effects of SFQSeM were evaluated in a *D*-galactose-induced oxidative stress model and an antibiotic-treated mouse model. SFQSeM supplementation significantly reduced the oxidative stress in *D*-galactose-treated mice. It also promoted the growth of beneficial bacteria and increased the levels of acetate, butyrate and lactate in the intestine ($P < 0.05$). In the antibiotic-treated mouse model, depletion of the intestinal microbiota significantly reduced hepatic glutathione peroxidase (GSH-Px) activity (26.6%) and glutathione peroxidase 1 (*GPx-1*) expression (48.77%) compared to normal mice supplemented with SFQSeM ($P < 0.05$). In contrast to Na_2SeO_3 and selenomethionine, SFQSeM effectively restored the diversity of the intestinal microbiota disrupted by antibiotics. *Lactobacillus*, Lachnospiraceae_NK4A136_group, and Muribaculaceae were identified as predominant bacteria in the SFQSeM group, and were strongly associated with increased hepatic GSH-Px activity and *GPx-1* mRNA expression ($P < 0.05$). In conclusion, intestinal microbiota enhances the antioxidant efficacy of SFQSeM by modulating microbial composition, producing active metabolites, and converting SFQSeM into a bioactive form of selenium.

1. Introduction

Selenium is recognized for its significant antioxidant properties[1]. Its principal mechanism of action in mitigating oxidative stress involves the synthesis of selenoproteins, including glutathione peroxidase (GPx), thioredoxin reductase (TXNRD), and iodothyronine deiodinase (IDD)[2-4]. These selenoproteins play a critical role in enhancing antioxidant defenses, making them essential for combating oxidative stress and maintaining cellular health[5]. Selenium occurs naturally in the inorganic forms of selenite (SeO_3^{2-}) and selenate (SeO_4^{2-}), and in organic forms including selenomethionine (SeM), selenocysteine (SeC) and Se-polysaccharide in nature. Currently, traditional selenium supplementations (mainly as Na_2SeO_3 and SeM), although shown to have some benefits, has also been associated with toxicities[6]. Food-derived selenium-containing peptides have emerged as promising selenium carriers. They offer dual benefits by combining the bioactive properties of peptides and selenium, as well as safety of consumption[7]. Increasing evidence shows that selenium plays a key role in the antioxidant capacity of the peptides. For instance, SeMet-Pro-Ser was superior to Met-Pro-Ser in terms of stability and antioxidant activity[8]. Se-enriched *Cordyceps militaris* peptides demonstrated enhanced neuroprotection properties compared to *C. militaris* peptides[9]. However, the relationship between selenium metabolism and the antioxidant activity of selenium-containing peptides *in vivo* remains unclear.

* Corresponding authors.
E-mail address: luchenyang@nbu.edu.cn (C.Y. Lu); huangshaohua@nbu.edu.cn (S.H. Huang)
Peer review under responsibility of Beijing Academy of Food Sciences.

SciOpen Publishing services by Tsinghua University Press

http://doi.org/10.26599/FSHW.2025.9250494

Recent studies have highlighted the significant influence of selenium on the intestinal microbiota[10]. Selenium supplementation has shown a beneficial effect in promoting a healthy intestinal microbiota, which has the potential to ameliorate the intestinal microbiota ecosystem and subsequently impact host metabolism and immune activity[11-12]. Selenium levels and its chemical forms exhibit different influence on intestinal microbiota composition. Ferreira et al.[12] suggested that both organic and inorganic selenium supplementation in dog diets promoted the abundance of Lachnospiraceae, *Holdemanella*, and Ruminococcaceae UCG-014. Dogs fed with organic selenium displayed higher total production of volatile fatty acids in feces, particularly elevated the concentrations of propionic and butyric acids compared to inorganic selenium-fed dogs. This result suggests a superior regulatory effect of organic selenium on the intestinal microecology compared to inorganic selenium[13]. In our previous studies, a selenium-containing peptide from soybean (SePPs) was prepared, which showed superior antioxidant and anti-inflammatory effects *in vivo* compared to inorganic selenium (Na_2SeO_3) and selenoamino acid (SeM)[14]. A tetrapeptide Ser-Phe-Gln-SeM (SFQSeM) identified from SePPs has demonstrated remarkable intracellular antioxidant and anti-inflammatory efficacy. However, in an *in vitro* small intestinal absorption model, SFQSeM showed a significantly lower translocation rate when compared to SeM and Na_2SeO_3[15].

We therefore hypothesize that intestinal microbiota significantly alters the host metabolism of SFQSeM *in vivo* and improves the antioxidant status of the host. To address this, we used a *D*-galactose (*D*-gal)-induced oxidative stress model to evaluate the systemic antioxidant responses to SFQSeM, as this model mimics aging by chronic oxidative stress *in vivo* and is closely associated with the intestinal microbiota[16]. Additionally, an antibiotic-treated mouse model was used to explore microbiota-dependent antioxidant mechanisms by depleting intestinal microorganisms[17], thereby isolating their specific contribution to the effects of SFQSeM. The impacts of different selenium compounds on intestinal microbiota systems were also studied in both normal mice and antibiotic-treated mice. We seek to deepen the understanding of the interactions between the host metabolism of selenium-containing peptides and the intestinal microbiome, potentially unlocking its full therapeutic potential.

2. Materials and methods

2.1 Materials

Chemicals (Na_2SeO_3, SeM, *D*-gal) were purchased from Sigma Chemical Co. (St. Louis, MO, USA). All kits (for aspartate aminotransferase (AST), alanine aminotransferase (ALT), glutathione peroxidase (GSH-Px), superoxide dismutase (SOD), total antioxidant capacity (T-AOC), and reduced glutathione (GSH)) were purchased from Nanjing Jiancheng Bioengineering Institute (Nanjing, China). Antibiotics of cefixime, ampicillin and clindamycin were purchased from Hunan Xiangya Pharmaceutical Co., Ltd. (Hunan, China), Haikou Qili Pharmaceutical Co., Ltd. (Haikou, China) and Jiudian Pharmaceutical Co., Ltd. (Hunan, China). Tetrapeptide SFQSeM were synthesized from Hefei Guotai Foods Co., Ltd. (Hefei, China) with a purity of 98%.

2.2 Animal studies

All animal works were carried out in the Laboratory Animals of Huazhong Agricultural University in specific pathogen-free (SPF) conditions with controlled temperature ((22 ± 2) ℃) and a 12 h light-12 h dark photoperiod.The mice were purchased from Hunan SJA Laboratory Animal Co., Ltd. (Hunan, China) under the animal production license number SCXK (Xiang) 2019-0004. The animals were provided with a standard diet obtained from Trophic Animal Feed High-Tech Co., Ltd. (Nantong, China). Mice were acclimated to the surrounding for one week before treatment. All the procedures performed were approved by the Guidelines for Care and Use of Laboratory Animals of Huazhong Agricultural University and the animal ethics approving number was HZAUMO-2021-0175.

D-Gal induced oxidative stress model: The *D*-gal-treated mouse model was established according to previous study with slight modification[18]. Thirty female ICR mice ((18 ± 1) g) were randomly divided into 3 groups (n = 10). The *D*-gal and SFQSeM group were pretreated with the intraperitoneal injection of *D*-gal (250 mg/kg body weight) for 4 weeks. Meanwhile, the control group received the same amount of normal saline. They were fed with normal saline (control and *D*-gal groups) or SFQSeM diet (SFQSeM group, 0.25 mmol/(L·kg body weight)) for the last four weeks. Serum, liver, brain and caecum were collected at sacrifice by cervical dislocation and stored at –80 °C until analysis. Oxidation levels including serum T-AOC and GSH, and hepatic SOD, GSH-Px, ALT and AST were quantified by kits following the manufacturers' instructions. Liver tissues were homogenized in precooled TRIzol and RIPA lysate for mRNA analysis. Caecum was utilized for intestinal microbiome analysis.

Antibiotic induced intestinal microbiota inhibition model: the antibiotic-treated mouse model was established according to previous study with slight modification[17]. Forty male Kunming mice ((20 ± 2) g) were randomly divided into 8 groups (n = 5), in which four groups were pretreated with a cocktail of antibiotics (cephalexin:ampicillin: clindamycin = 3:10:5) for 5 days. Meantime, the other four groups were given equal volume of normal saline. Five days after antibiotic treatment, mice were given the corresponding selenium supplements: selenium-deficient diet (normal saline, selenium concentration < 0.01 mg/L), Na_2SeO_3, SeM and SFQSeM diet. All selenium treatments were administered via oral gavage, providing a final selenium intake of 60 μg/kg body weight per day. Five days after the final selenium treatment, mice were sacrificed 5 days after the final selenium treatment. Serum, liver and caecum were collected and stored at –80 °C until analyzed. Total selenium levels in serum were determined with the atomic fluorescence spectroscopy (AFS) system. Liver tissues were homogenized in precooled TRIzol and RIPA lysate for mRNA analysis. Caecum were utilized for intestinal microbiome analysis.

2.3 Determination of total Se concentration

Total Se concentrations in the liver and serum were detected by an SA-50 atomic fluorescence spectrometer (AFS) (Titan Instruments Co., Ltd., Beijing, China) in accordance with the standards for the determination of Se in foods established by the People's Republic of China (GB 5009.93-2017).

2.4 Histological examination

Left liver lobes (approximately 1 cm × 1 cm × 0.2 cm in size) were dissected and fixed in 4% paraformaldehyde for 24 h. The tissue was processed by a standard paraffin embedding procedure and sectioned at 5 μm. Sections were stained with haematoxylin to visualise nuclei. After a brief differentiation step using a weak acid alcohol solution to remove excess haematoxylin, the slides were stained with eosin using an alcoholic eosin solution. To ensure complete dehydration and transparency, the stained slides were washed twice with alcohol to remove any residual water.

2.5 Quantitative analysis of gene expressions

Quantitative real-time polymerase chain reaction (qPCR) analysis was used to measure the gene expressions of selenoproteins, inflammatory factor and antioxidant gene expression in liver and kidney. RNA was extracted from frozen liver and kidney using the TRIzol reagent (Thermo Fisher Scientific, US). The cDNA was reverse transcribed using a Reverse Transcription System Kit (Thermo Fisher Scientific, US). qPCR was performed on an 7500 real-time PCR system (ABI, UK) using SYBR green select master mix (Thermo Fisher Scientific, US). Primers were designed using Primer3 and synthesized by Qinke Biotech Co., Ltd. (Shanghai, China). Relative quantification was achieved using the ΔΔCt method and mice β-actin was used as a housekeeping gene.

2.6 Determination of quantification of short-chain fatty acids

Caecum samples ((1.000 ± 0.100) g) were homogenized with 2 mL of ultrapure water on ice and centrifuged at 14 000 × *g* for 10 min. The obtained supernatants were mixed with 0.5 mL 50% H_2SO_4, following by adding 1 mL diethyl ether. The mixture rest for 30 min on ice, and then centrifuged for 10 min at 14 000 × *g*. The supernatants were filtered by using a 0.22 μm RC filter before injection to gas chromatograph (GC). The analytes were injected in samples (1.0 μL) into a SHIMADZU GC2010 GC system (Kyoto, Japan). The oven temperature was programmed to start at 90 °C (5 min), to increase to 96 °C at 3 °C/min, and then to increase to 220 °C for 10 °C/min. The standard solutions of acetic, propionic, butyric and lactic acid were considered in the evaluation of theanalytic method.

2.7 Microbiota characterization

Total genomic DNA was extracted using DNA extraction kit following the manufacturer's instructions. The genomic DNA was used as a template for PCR amplification using the barcoded primers and Tks Gflex DNA Polymerase (TaKaRa). For bacterial diversity analysis, the V3-V4 variable regions of 16S rRNA genes were amplified using universal primers 343F and 798R (or 515F and 907R for V4-V5 regions). Amplicon quality was visualised by gel electrophoresis, purified with AMPure XP beads (Agencourt) and amplified for a further round of PCR. After further purification with AMPure XP beads, the final amplicon was quantified using the Qubit dsDNA assay kit. Equal amounts of purified mplicon were pooled for subsequent sequencing. Clean reads were subjected to primer sequence removal and clustering to generate operational taxonomic units (OTUs) using Vsearch software with a 97% similarity cutoff. The representative read of each OTU was selected using the QIIME package. All representative reads were annotated and compared to Silva database version 123 (or Greengens) (16S/18S rDNA) using RDP classifier (confidence threshold was 70%).

2.8 PICRUSt2 analysis

PICRUSt2 (Phylogenetic Investigation of Communities by Reconstruction of Unobserved States) software (version 2.3.0) was used to predict functional gene composition. The software annotates the characteristic sequences of each sample against a phylogenetic tree, using the IMG microbiome database (version 5.0) for functional gene output. STAMP (Statistical Analysis of Metagenomic Profiles, version 2.1.3) software was used to assess significant differences in functional abundance between different groups. KEGG (Kyoto Encyclopedia of Genes and Genomes, version 91) pathway analysis was performed to compare differences in metabolic pathways between groups, providing insight into how microbial communities may adapt their metabolic functions in response to environmental changes. Pairwise comparisons between groups were performed using a two-tailed *t*-test with a significance threshold of $P < 0.05$.

2.9 Data analysis

Pearson's correlation analysis was performed using SPSS Statistics (version 19.0, IBM Corp.) software, The significance level for the correlation was set at $P < 0.05$. All data were presented as mean values with standard deviations. Statistical analysis was performed using One-way analysis of variance (ANOVA) in the SPSS 19.0 software. Significance levels were determined by one-way ANOVA followed by a *post hoc* Tukey's HSD test for multiple comparisons at $P < 0.05$.

3. Results

3.1 SFQSeM treatment ameliorated the antioxidant status in D-gal-treated mice

To investigate the antioxidant activity of SFQSeM *in vivo*, a *D*-gal-induced mouse oxidative stress model (Fig. 1A) was established in this study. As shown in Figs. 1B-H, after 8 weeks of intraperitoneal injection of *D*-gal, the total antioxidant capacity T-AOC, GSH and SOD levels in mouse serum, and the GSH-Px and SOD levels in mouse liver were significantly reduced, while liver ALT and AST levels were significantly increased compared with the control group ($P < 0.05$). These results indicate that *D*-gal injection resulted in decreased antioxidant levels and impaired hepatic function in mice, and supplementation with SFQSeM helped to restore these serum and hepatic antioxidant indicators to normal levels.

The micrograph of hematoxylin-eosin (H&E) staining of mouse liver is shown in Figs. 2A-C. Significant inflammatory cell infiltration was observed in the *D*-gal group, and the inflammatory factor level of necrosis factor-alpha (TNF-α) was found to be significantly higher than that in the normal mice ($P < 0.05$, Fig. 2F). In the SFQSeM group, inflammatory cell infiltration was improved and its tissue distribution was similar to that of the control group. SFQSeM treatment significantly increased the mRNA level of *GPx-1* and

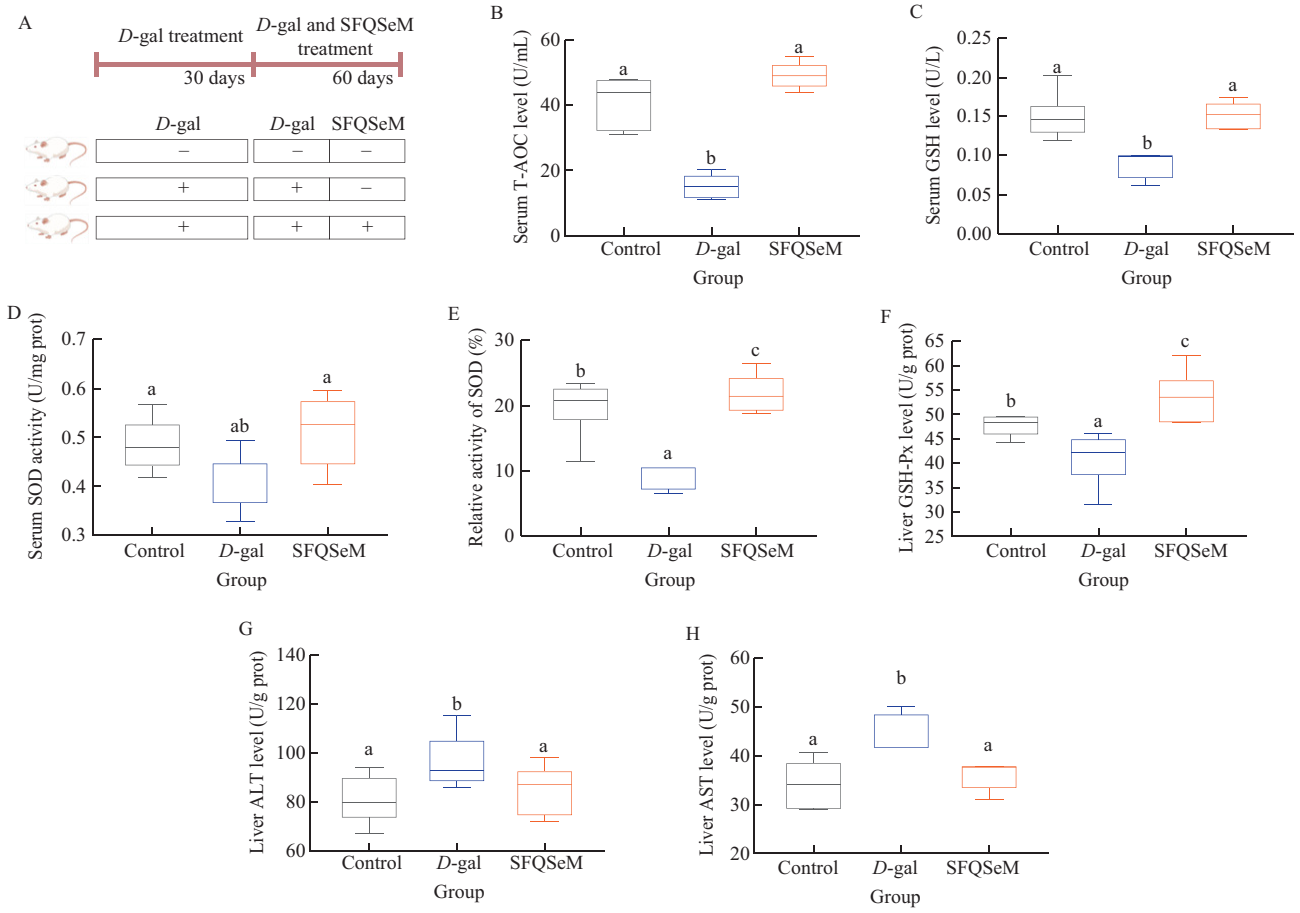

Fig. 1 SFQSeM treatment ameliorated the antioxidant status of *D*-gal induced oxidative stress. (A) Flowchart of *D*-gal-induced oxidative stress model. Mouse serum T-AOC (B), GSH (C) and SOD (D) levels. Liver SOD (E), GSH-Px (F), ALT (G) and AST (H) levels. Different letters indicate significant differences among groups ($P < 0.05$).

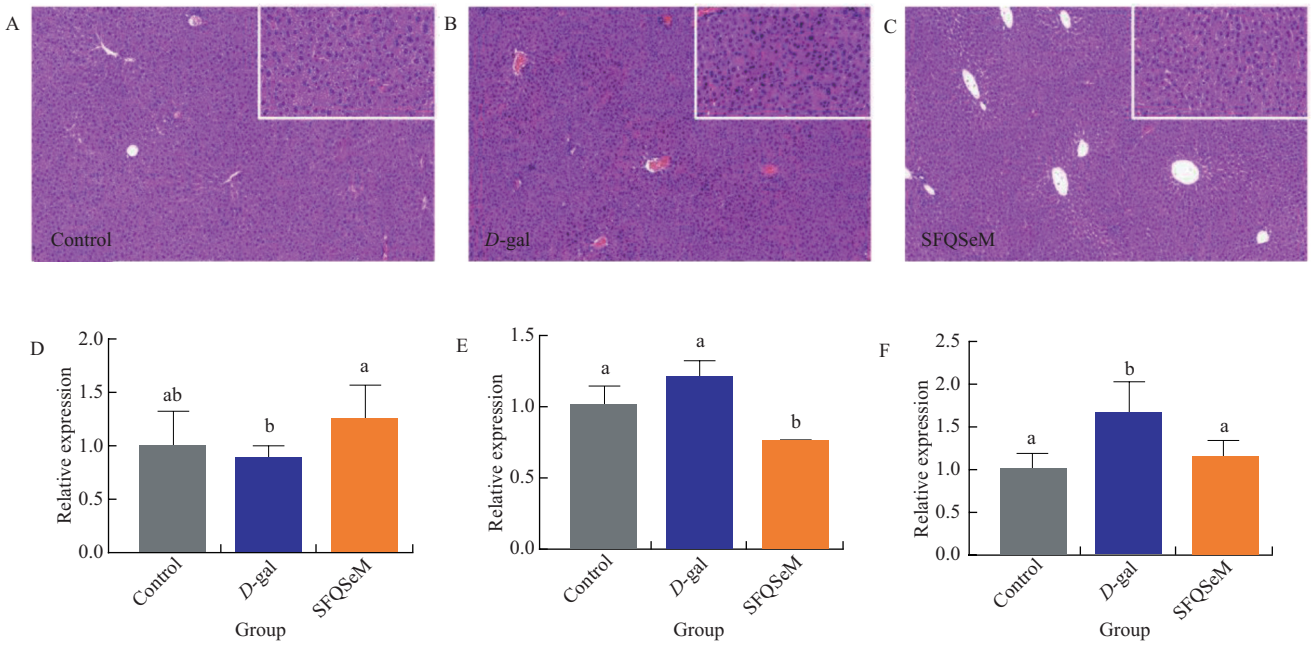

Fig. 2 H&E staining of and expression levels of antioxidant-related genes in the liver of *D*-gal-treated mice. Representative H&E staining images of mice in control (A), *D*-gal (B) and SFQSeM (C) treated groups. The gene expression levels of *GPx-1* (D), *NF-κB* (E) and *TNF-α* (F). Different letters indicate significant differences among groups ($P < 0.05$).

markedly decreased the mRNA levels of nuclear factor-kappa B (*NF-κB*), *TNF-α* ($P < 0.05$), thus protecting the hepatocytes from the *D*-gal-induced oxidative stress (Figs. 2D-F).

3.2 SFQSeM treatment affects intestinal microbiota structure in D-gal-induced ageing mice

To further investigate how SFQSeM reversed the progression of the antioxidant status in mice, particularly the metabolic changes in the intestinal microbiota, we performed an intestinal microbiota analysis of mouse caecum samples. As shown in Fig. 3A, an increased abundance of Firmicutes followed by a decreased abundance of Bacteroidetes was observed in mice infected with *D*-gal. These results are supported by previous studies that suggested an increased Firmicutes to Bacteroidetes ratio in aged mice compared to young adult mice[19]. SFQSeM supplementation was beneficial in reducing the elevated Firmicutes to Bacteroidetes ratio. At the genus level, SFQSeM group showed a trend toward increasing *Bacteroides* and decreasing *Helicobacter* and *Roseburia* compared to the *D*-gal group, although these changes did not reach statistical significance ($P > 0.05$). In particular, a significant higher abundance of *Lactobacillus* was observed in mice fed SFQSeM (Fig. 3B, $P < 0.05$). The Pearson's correlation analysis showed that *Lactobacillus* and Muribaculaceae exhibited positive correlations with serum SOD activity and hepatic SOD activity. While Rikenellaceae_RC9_gut_group and *Bacteroides* were negatively correlated with liver SOD activity and surm GSH level (Fig. S1, $P < 0.05$).

As shown in Figs. 3C-E, *D*-gal injection did not significantly affect the levels of, butyrate and lactic acid compared with the normal group ($P < 0.05$). However, SFQSeM intake induced a remarkable increase in acetate, butyrate and lactic acid levels ($P < 0.05$).

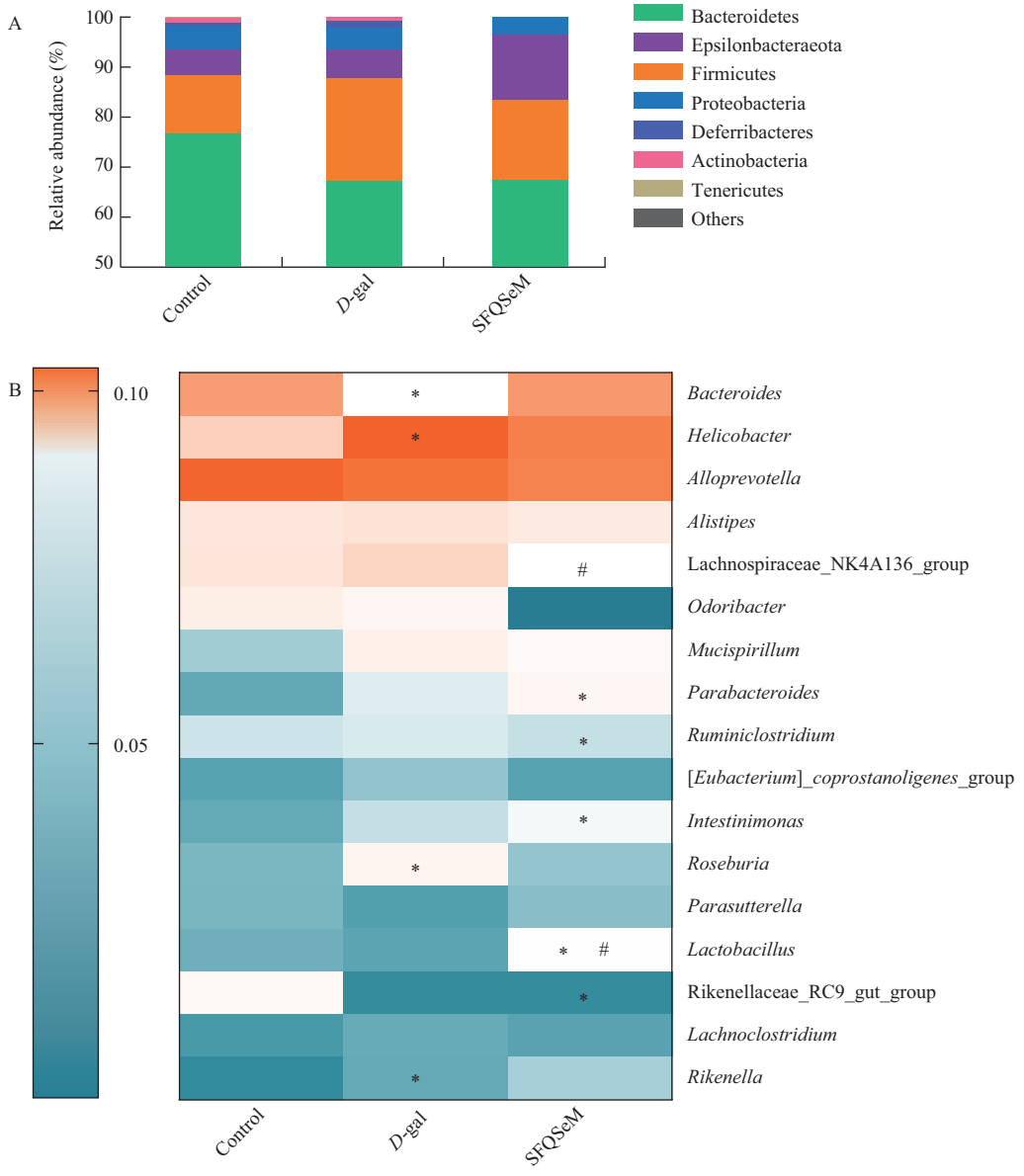

Fig. 3 SFQSeM treatments regulated intestinal microbial structure and intestinal microbial metabolites in *D*-gal-treated mice. (A) The relative abundance of the top 10 intestinal microbial phyla. (B) Heat map of taxa in the three groups at the genus level. Significant difference between control and *D*-gal groups are marked with $*P < 0.05$. Significant difference between control and other groups are marked with $^{\#}P < 0.05$. The level of acetate (C), butyrate (D) and lactic acid (E) in mice cecum. Different letters indicate significant differences among groups ($P < 0.05$).

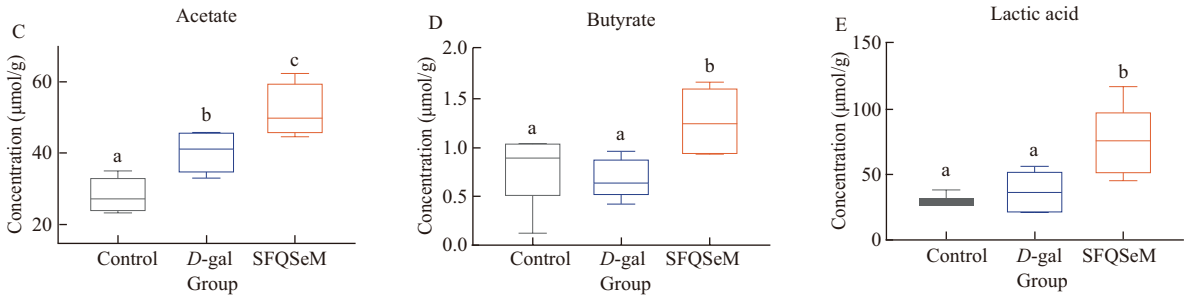

Fig. 3 (*Continued*)

3.3 Effects of intestinal microbiota on the metabolism of selenium compounds

3.3.1 Total selenium levels in mice serum

To understand the role of intestinal microbiota in converting different selenium compounds, we employed an antibiotic-treated mice model (Fig. 4A) by using a combination of antibiotics including ampicillin, clindamycin, and cefoperazone to suppress the intestinal microbiota[20-21]. As shown in Fig. 4B, following the supplementation with Na_2SeO_3, SeM, and SFQSeM, there was a significant increase in serum selenium levels in both normal and antibiotic-treated mice ($P < 0.05$). Serum selenium levels in the Na_2SeO_3 and SeM groups were significantly higher than those in the SFQSeM groups ($P < 0.05$). There was no significant difference between the antibiotic-treated mice and the normal mice within each selenium supplementation group ($P > 0.05$).

3.3.2 GSH-Px activity in mice serum and liver

GSH-Px activity serves as a crucial indicator of the bioavailability of selenium compounds[22]. The effect of intestinal microbiota on GSH-Px activity was examined in both the liver and serum. In the liver, the supplementation with SeM and SFQSeM significantly increased the GSH-Px activity in normal mice ($P < 0.05$), whereas Na_2SeO_3 showed no significant effect on GSH-Px activity ($P > 0.05$) (Fig. 4C). Particularly, in the SeM treatment groups, the hepatic GSH-Px activity of antibiotic-treated mice was significantly higher than that in the normal mice ($P < 0.05$). However, in the SFQSeM treatment group, the GSH-Px activity of normal mice was noticeably higher than that of antibiotic-treated mice ($P < 0.05$). Similarly, the supplementation with organic selenium SeM and SFQSeM significantly elevated GSH-Px activity in normal mice serum ($P < 0.05$, Fig. 4D). However, in antibiotic-treated mice, only the SeM group showed a significant increase in GSH-Px activity ($P < 0.05$). Additionally,

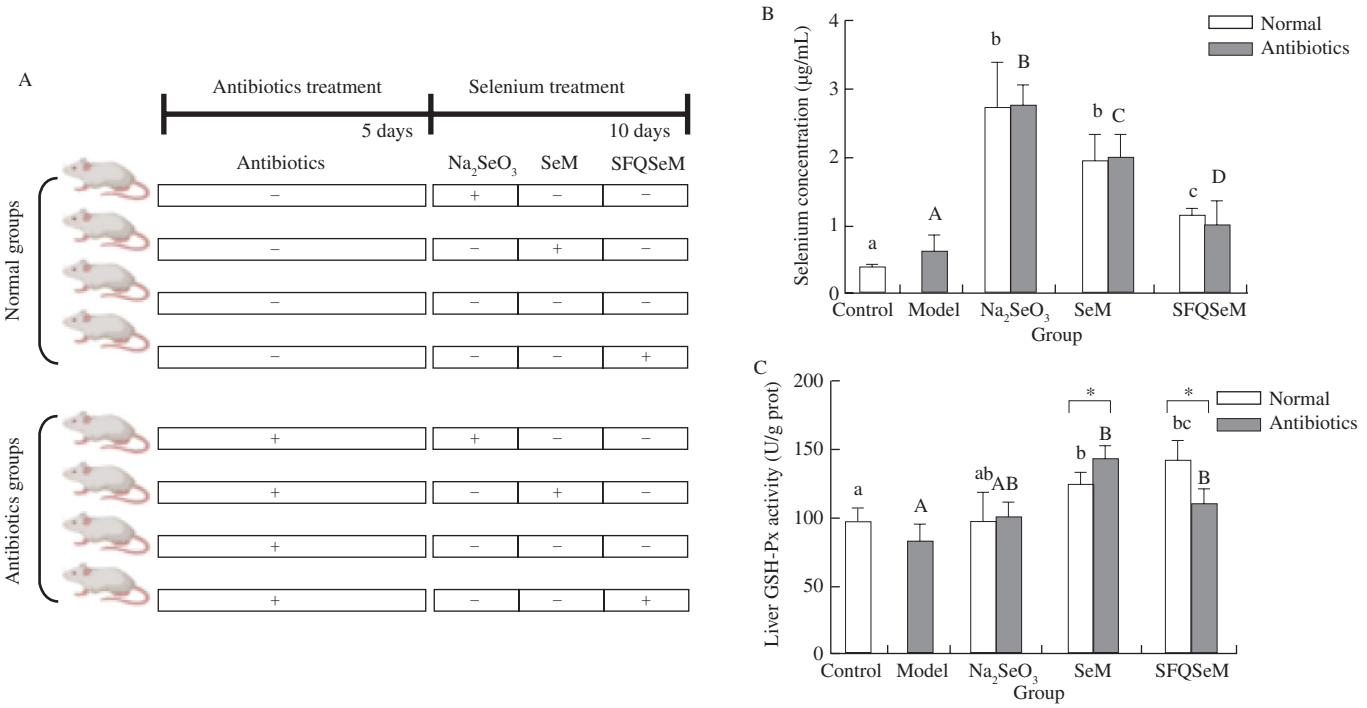

Fig. 4 Impact of selenium supplementation on selenium metabolism and antioxidant function markers in serum and liver of normal and antibiotic-treated mice. (A) Flowchart of experimental animal models in normal and antibiotic-treated mice; (B) selenium concentration in mice serum; (C) GSH-Px activity in liver; (D) GSH-Px activity in serum. Selenoprotein expression in the liver. mRNA expression of *GPx-1* (E), *TXNRD1* (F) and *Sepp1* (G) in liver. a, b, c, d indicates significant differences between columns in normal mice that do not share letters. A, B, C, D indicates significant differences between columns in antibiotic-treated mice that do not share letters. * indicates a significant difference between normal and antibiotic group. Statistical significance was determined using one-way ANOVA followed by a *post hoc* Tukey's HSD test for multiple comparisons ($P < 0.05$).

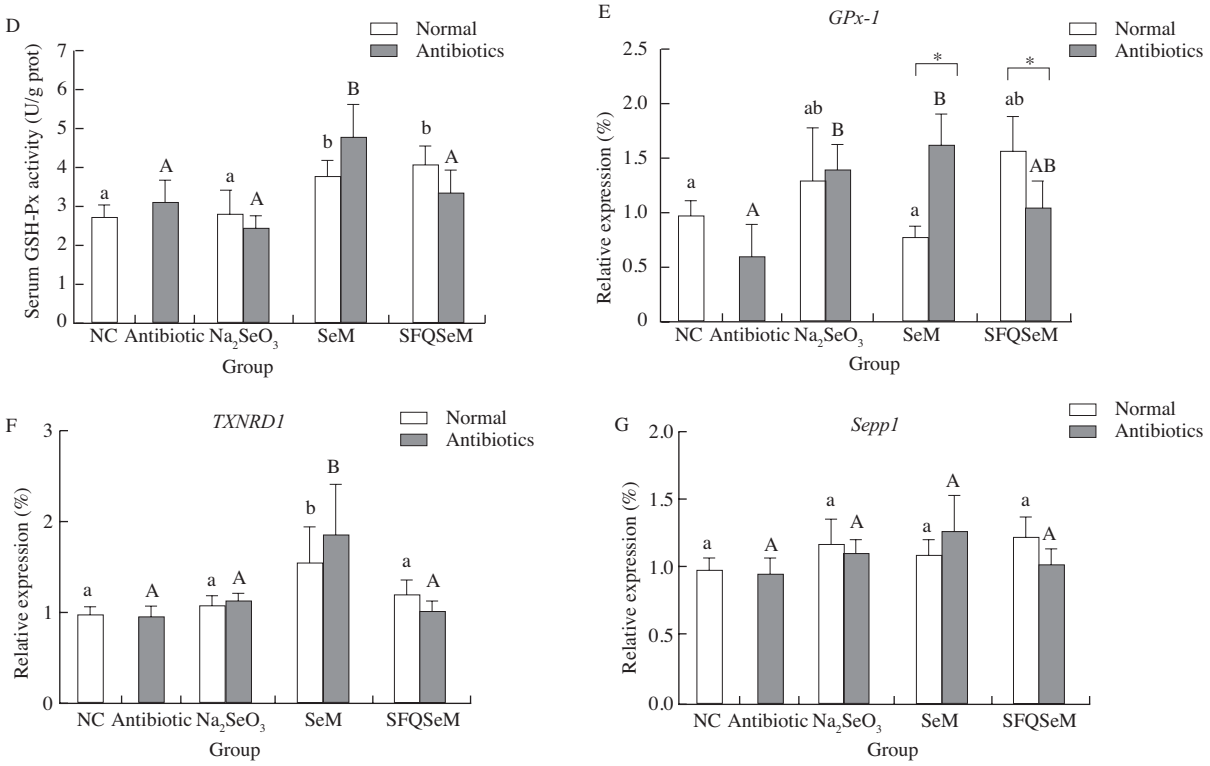

Fig. 4 (*Continued*)

in the SeM group of antibiotic-treated mice, GSH-Px activity was higher than that in normal mice. In the SFQSeM group of normal mice, GSH-Px activity was higher than that in antibiotic-treated mice, although these effects did not reach statistical significance ($P > 0.05$).

3.3.3 Selenoprotein expressions in mice liver

Gene expression of the essential selenoproteins *GPx-1*, *TXNRD1* and *Sepp1* in the liver is shown in Figs. 4E-G. In normal groups, no significant changes in hepatic *GPx-1* mRNA levels were observed when compared to the control, Na_2SeO_3, SeM and SFQSeM groups ($P > 0.05$). In the antibiotic-treated groups, supplementation with Na_2SeO_3 and SeM significantly increased *GPx-1* gene expression compared to the antibiotic group ($P < 0.05$). Furthermore, the *GPx-1* mRNA expression in antibiotic-treated mice was notably higher than that in normal mice after SeM supplementation ($P < 0.05$), while the *GPx-1* mRNA expression in normal mice was significantly higher than that in antibiotic-treated mice after SFQSeM supplementation (Fig. 4E, $P < 0.05$). As shown in Fig. 4F, in both normal and antibiotic-treated mice, *TXNRD1* expression increased significantly only in the SeM group ($P < 0.05$). There was no significant effect on hepatic *Sepp1* mRNA expression among Na_2SeO_3, SeM and SFQSeM groups in both normal and antibiotic-treated mice (Fig. 4G, $P > 0.05$).

3.4 Effect of antibiotic and selenium supplementation on the intestinal microbiota

3.4.1 Modulation of different selenium compounds on intestinal microbiota diversity

As shown in Figs. 5A-C, antibiotic intervention significantly reduced the α-diversity indexes (Chao1, Shannon, and Simpson) of the intestinal microbiota ($P < 0.05$). The Shannon and Simpson indices returned to normal levels after SFQSeM supplementation. In normal mice, SeM notably decreased Shannon and Simpson indices ($P < 0.05$), indicating an impact on intestinal microbiota diversity. The β-diversity analysis among selenium-supplemented groups in both normal and antibiotic-treated mice is illustrated in Figs. 5D and E. In the normal mice, principal coordinate analysis (PCoA) revealed significant differences between the Na_2SeO_3, SeM and SFQSeM groups compared to the normal group, with SeM showing the most distinct (Fig. 5D). In antibiotic-treated mice, significant differences were observed between the normal groups and the antibiotic-treated groups, whereas SFQSeM supplementation enabled mice in the antibiotic-treated group to have a microbiota structure closer to that of the normal group (Fig. 5E).

3.4.2 Modulation of different selenium compounds on intestinal microbiota composition

As shown in Figs. 5F-I, in normal mice, the predominant taxa in the caecum were Bacteroidetes and Firmicutes at the phylum level. Following antibiotic intervention, the abundance of both Bacteroidetes and Firmicutes decreased significantly, while Proteobacteria became the dominant taxa in the antibiotic model group ($P < 0.05$). After the supplementation with SFQSeM in antibiotic-treated mice, Bacteroidetes, Firmicutes, and Proteobacteria abundances approached normal levels. In normal selenium-supplemented mice, SeM intake significantly reduced the abundance of Bacteroidetes, elevated the abundance of Proteobacteria ($P < 0.05$), suggesting that SeM might also induce the intestinal microbiota dysbiosis.

The relative abundance of the bacterial community and part of the microbiota at the genus level are shown in Fig. 6. There was a significant increase in *Akkermansia*, *Lactobacillus*, *Butyricioccus*,

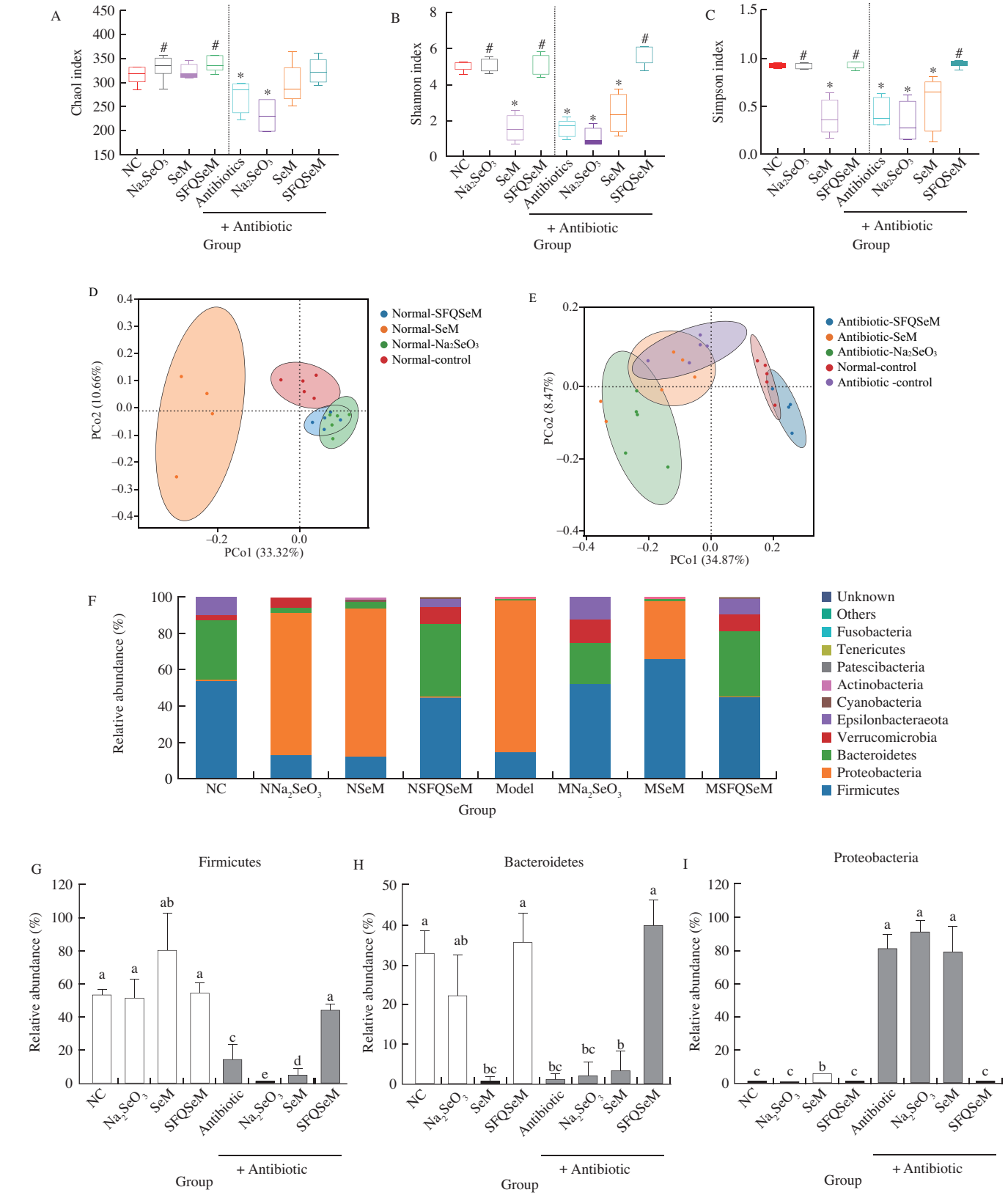

Fig. 5 Effects of different selenium compounds on the profile of intestinal microbiota. α-Diversities of Chao1 (A), Shammon (B) and Simpson (C) in normal mice and antibiotic-treated mice; β-diversity of the intestinal flora in normal mice (D) and antibiotic-treated mice (E). Modulation of intestinal flora composition at phylum levels by different selenium compounds (F). Groups are defined as follows: NC, NNa_2SeO_3, NSeM, and NSFQSeM represent mice treated with normal saline followed by administration of saline, Na_2SeO_3, SeM, and SFQSeM, respectively. Model, MNa_2SeO_3, MSeM, and MSFQSeM represent mice treated with antibiotics followed by the same respective selenium supplements. Changes in the distribution of intestinal flora of Firmicutes (G), Bacteroidetes (H) and Proteobacteria (I). * indicates a significant difference between NC and other groups, # indicates a significant difference between antibiotic group and other groups. Statistical significance was determined using One-way ANOVA followed by a *post hoc* Tukey's HSD test for multiple comparisons ($P < 0.05$).

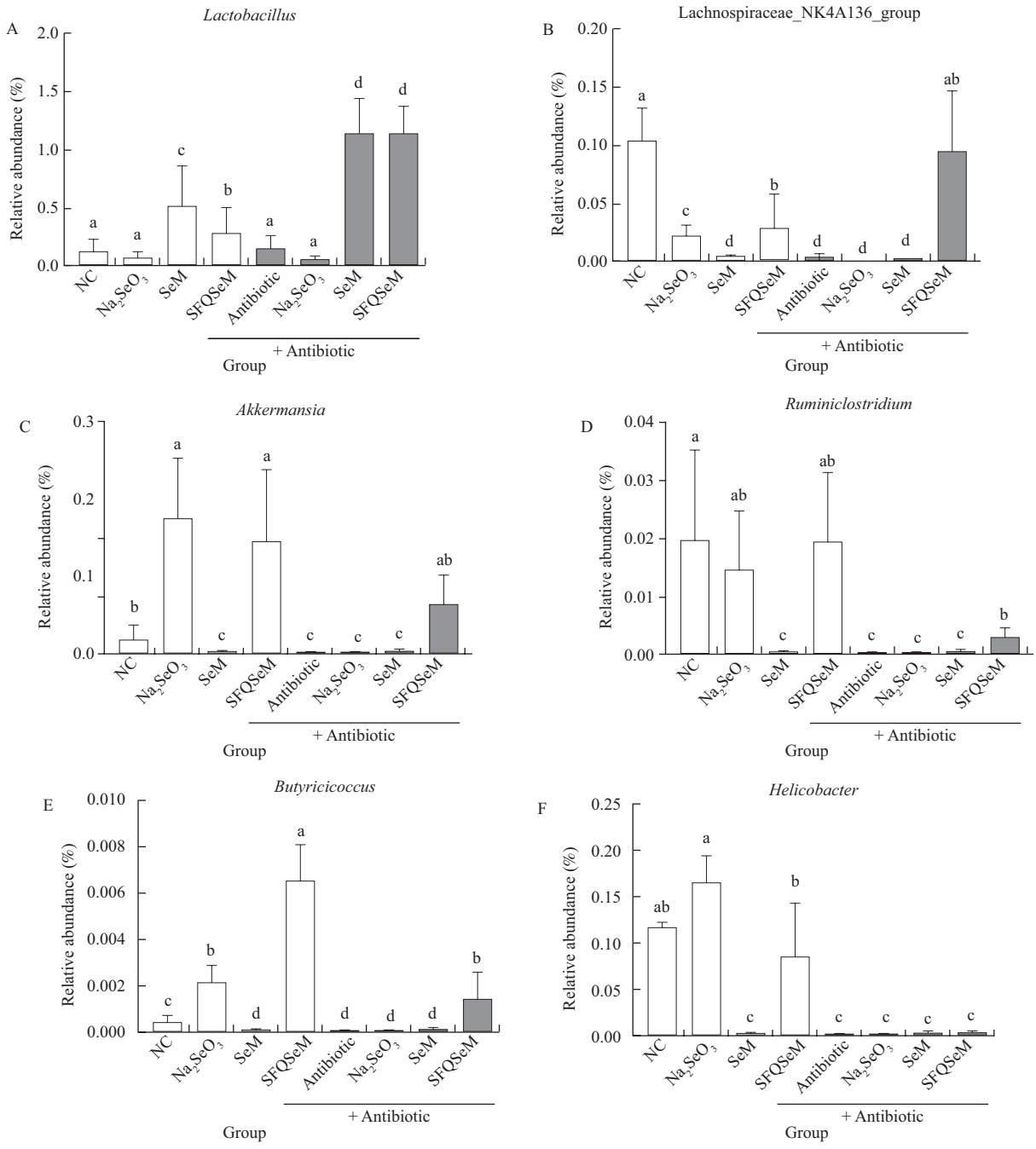

Fig. 6 Modulation of intestinal microbiota composition at gene levels by different selenium compounds. Changes in the distribution of intestinal flora of *Lactobacillus* (A), Lachnospiraceae-NK4A136-group (B), *Akkermansia* (C), *Ruminiclostridium* (D), *Butyricioccus* (E), *Helicobacter* (F). $^{a, b, c, d}$ indicates significant differences between columns in normal mice that do not share letters. Statistical significance was determined using one-way ANOVA followed by a *post hoc* Tukey's HSD test for multiple comparisons ($P < 0.05$).

Lachnospiraceae-NK4A136 group and *Ruminiclostridium* abundance in antibiotic-treated mice supplemented with SFQSeM ($P < 0.05$). The SeM groups also had significantly higher levels of *Lactobacillus* than the NC group ($P < 0.05$), suggesting a remarkable effect of organic selenium compounds on the abundance of *Lactobacillus*.

In normal mice groups, linear discriminant analysis Effect Size (LEfSe) analysis showed that *Ruminiclostridium*, *Akkermansia*, *Helicobacter* were the dominant bacteria in the Na_2SeO_3 group. *Bacillus* and *Stenotrophomonas* were the dominant bacteria in SeM group, whereas Muribaculaceae, Bacteroidales, *Lactobcillus* and Lachnospiraceae were the dominant bacteria in the SFQSeM group (Fig. 7A). In antibiotic-treated mice groups, *Stenotrophomonas* and Xanthomonadaceae were the most significantly different genera in the model group, while the Na_2SeO_3 group was characterized by a higher abundance

of *Enterobacter* and *Bacillus*. *Clostridioides* and *Pseudomonas* were the most significantly different genera in the SeM group, and Muribaculaceae, Lachnospiraceae and *Blautia* were the most significantly different genera in the SFQSeM group (Fig. 7B).

3.4.3 Effects of different selenium compounds on the intestinal SCFAs content

As shown in Figs. 8A-C, antibiotic treatment led to a significant decrease in the content of acetate, propionate, and butyrate in the cecum. Supplementation of antibiotic-treated mice with Na_2SeO_3, SeM and SFQSeM significantly increased acetic acid levels ($P < 0.05$, Fig. 8A). In addition, SFQSeM significantly increased butyric acid levels in antibiotic-treated mice ($P < 0.05$, Fig. 8C). However, there were no significant changes in the level of propionate among the selenium compound treatments ($P < 0.05$, Fig. 8B).

3.4.4 Predicted intestinal microbiota functions using PICRUSt

Through PICRUSt analysis, there were no functional abundance differences among the selenium treatment groups and the normal group (data not shown). As shown in Figs. 8D-F, among the antibiotic-treated groups, the SFQSeM group showed significant higher abundance of pathways related to amino acid synthesis, secondary metabolite synthesis, metabolic pathways,

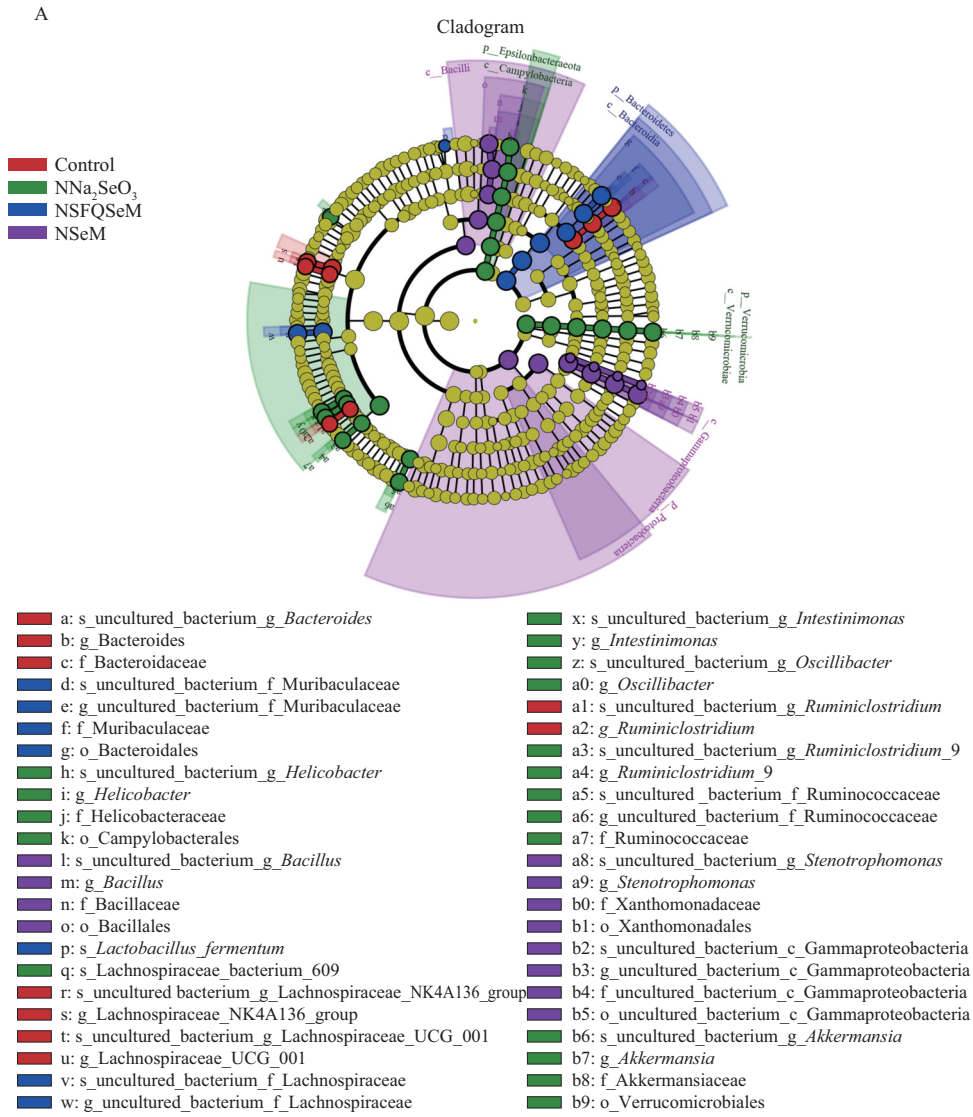

Fig. 7 LEfSe analysis of the mouse intestinal microbiota. LEfSe taxonomic cladograms showed the hierarchical relationships of the major taxonomic units from phylum to genus (from the inner circle to the outer circle) in (A) normal mice groups and (B) antibiotic-treated mice groups. Node size corresponds to the average relative abundance of the taxon. The colored nodes represent bacterial taxa that are significantly enriched in the corresponding groups (LDA score > 3.5), while yellow nodes represent taxa that do not differ significantly between groups. Groups are defined as follows: NC, NNa_2SeO_3, NSeM, and NSFQSeM represent mice treated with normal saline followed by administration of saline, Na_2SeO_3, SeM, and SFQSeM, respectively. Model, MNa_2SeO_3, MSeM, and MSFQSeM represent mice treated with antibiotics followed by the same respective selenium supplements. Abbreviations: p, phylum; c, class; o, order; f, family; g, genus.

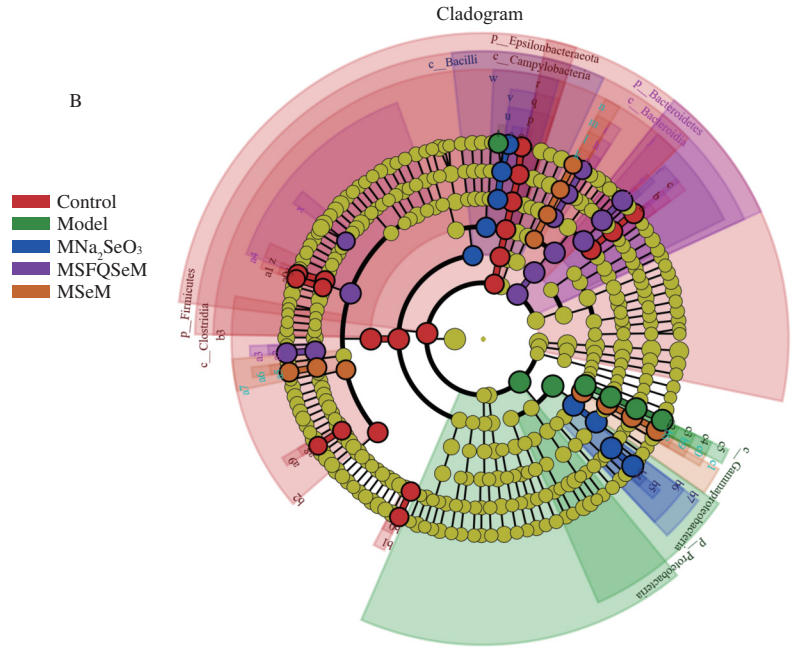

a: s_uncultured_bacterium_g_*Bacteroides*
b: g_*Bacteroides*
c: f_Bacteroidaceae
d: s_uncultured_bacterium_f_Muribaculaceae
e: g_uncultured bacterium_f_Muribaculaceae
f: f_Muribaculaceae
g: s_uncultured_bacterium_g_*Alistipes*
h: g_*Alistipes*
i: f_Rikenellaceae
j: o_Bacteroidales
k: s_uncultured_bacterium_g_*Elizabethkingia*
l: g_*Elizabethkingia*
m: f_Weeksellaceae
n: o_Flavobacteriales
o: s_uncultued_bacterium_g_*Helicobacter*
p: g_*Helicobacter*
q: f_Helicobacteraceae
r: o_Campylobacterales
s: s_*Bacillus circulans*
t: s_uncultured bacterium_g_*Bacillus*
u: g_*Bacillus*
v: f_Bacillaceae
w: o_Bacillales
x: g_*Blautia*
y: s_uncultured_bacterium_g_Lachnospiraceae_NK4A136_group
z: g_Lachnospiraceae_NK4A136_group
a0: s_uncultured_bacterium_g_Lachnospiraceae_UCG_001
a1: g_Lachnospiraceae_UCG_001
a2: s_uncultured_bacterium_f_Lachnospiraceae
a3: g_uncultured bacterium_f_Lachnospiraceae
a4: f_Lachnospiraceae
a5: s_*Clostridioides_difficile*
a6: g_*Clostridioides*
a7: f_Peptostreptococcaceae
a8: s_uncultured_bacterium_g_*Oscillibacter*
a9: g_*Oscillibacter*
b0: s_uncultured bacterium_f_Ruminococcaceae
b1: g_uncultured bacterium_f_Ruminococcaceae
b2: f_Ruminococcaceae
b3: o_Clostridiales
b4: s_uncultured_bacterium_g_*Enterobacter*
b5: g_*Enterobacter*
b6: f_Enterobacteriaceae
b7: o_Enterobacteriales
b8: s_uncultured_bacterium_g_*Pseudomonas*
b9: g_*Pseudomonas*
c0: f_Pseudomonadaceae
c1: o_Pseudomonadales
c2: s_uncultured_bacterium_g_*Stenotrophomonas*
c3: g_*Stenotrophomonas*
c4: f_Xanthomonadaceae
c5: o_Xanthomonadales

Fig. 7 (*Continued*)

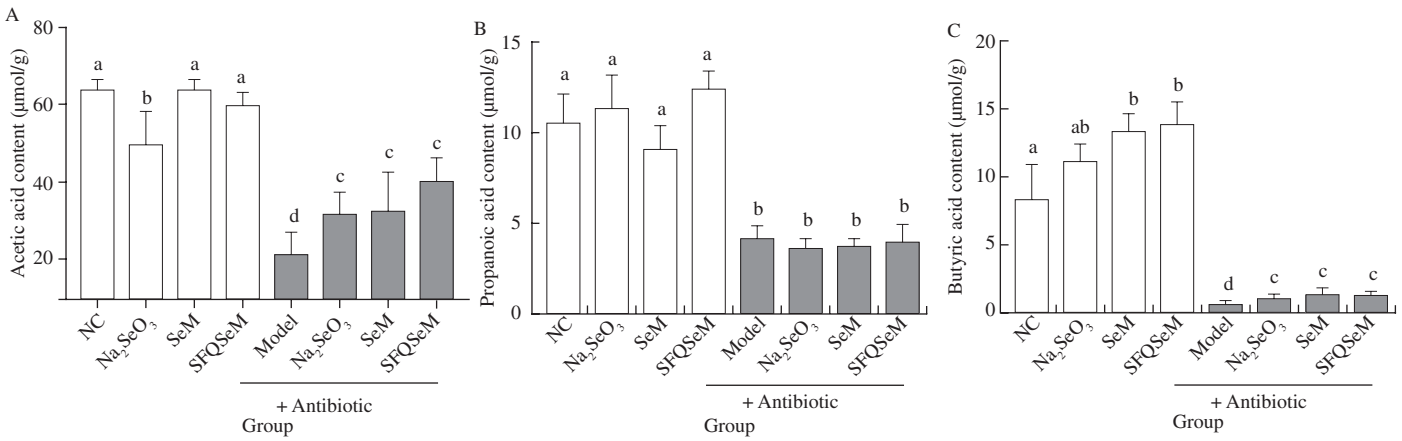

Fig. 8 Changes of metabolites and metabolic pathways of intestinal microbiota. Contents of acetic acid (A) propanoic acid (B) and butyric acid (C) in the cecum; PICRUSt analysis of intestinal flora between the model and SFQSeM groups (D), Na_2SeO_3 and SFQSeM groups (E), and SeM and SFQSeM groups (F) in antibiotic-treated mice. [a, b, c, d] indicates significant differences between columns in normal mice that do not share letters. Statistical significance was determined using One-way ANOVA followed by a *post hoc* Tukey's HSD test for multiple comparisons ($P < 0.05$).

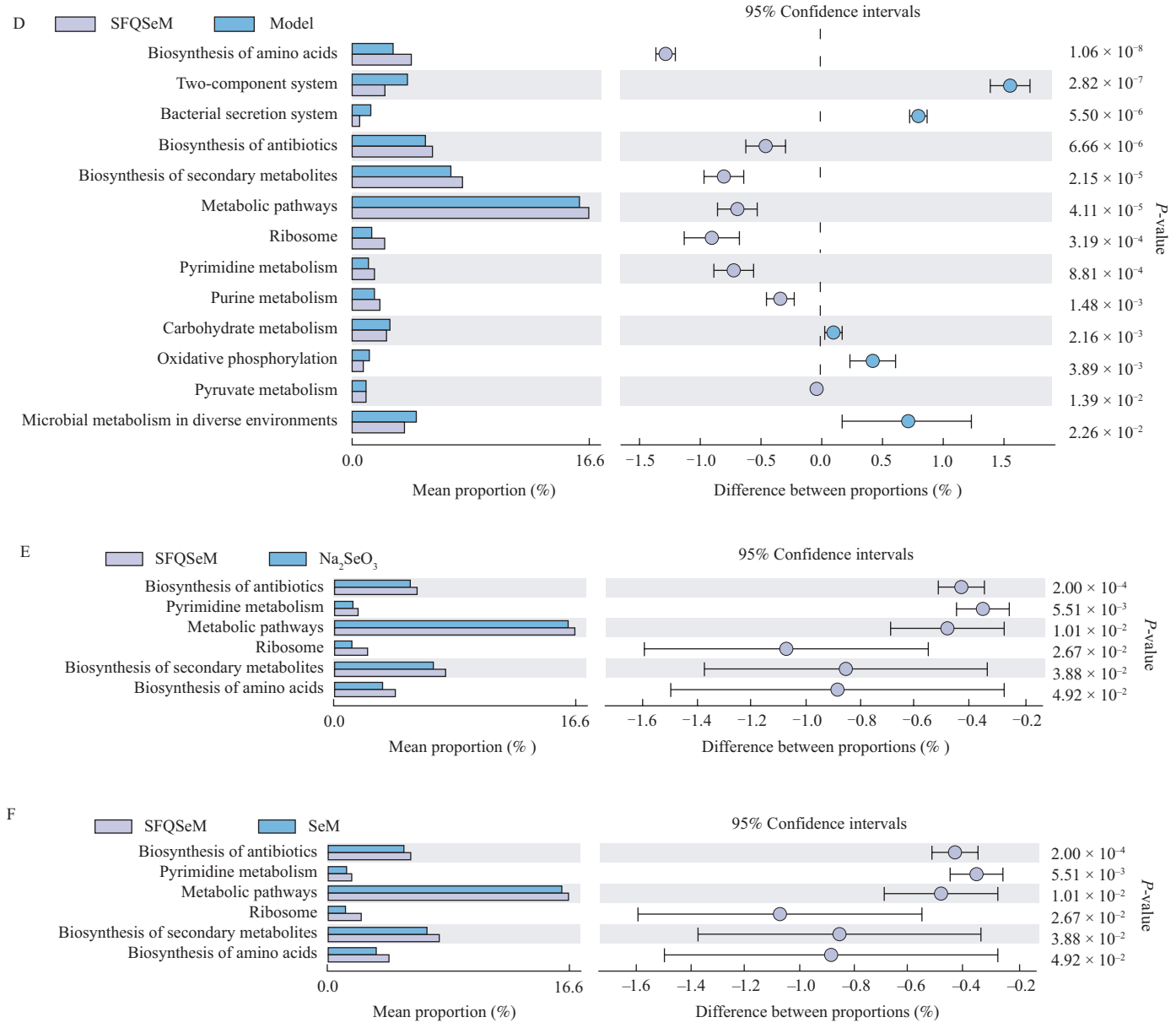

Fig. 8 (*Continued*)

ribosomes, pyrimidine and purine metabolism at KEGG level 3, in comparison with the model, Na_2SeO_3 and SeM groups. Simultaneously, there was a significant reduction in the abundance of pathways related to bacterial secretion systems, carbohydrate metabolism, and oxidative phosphorylation ($P < 0.05$).

3.4.5 Association of selenium metabolism and antioxidant function markers with intestinal microbiota

Pearson's correlation analysis was performed to investigate the correlations between selenium biomarkers and the relative abundance of specific bacteria. A significantly reduced number of associations was observed in the Na_2SeO_3 groups in normal and antibiotic-treated mice (Fig. S2). This may be explained by the reduced structural effects of the Na_2SeO_3 diet on the intestinal microbiota. In the normal mice (Figs. 9A and C), a higher abundance of the *Lactobacillus* was positively associated with serum selenium concentration in the normal SeM group, and with liver GSH-Px activity in the normal SFQSeM group. The promoted growth of *Akkermansia*, uncultured_bacterium_f_Muribaculaceae and uncultured_bacterium_f_Lachnospiraceae was positively associated with hepatic *GPx-1* expression in normal SFQSeM group. In the antibiotic-treated mice (Figs. 9B and D), positive correlations between GSH-Px activity in mice serum and *Clostridioides* were observed in SeM group, and positive correlations between GSH-Px activity in mice liver and uncultured_bacterium_f_Lachnospiraceae, Lachnospiraceae_NK4A136_group and uncultured_bacterium_f_Muribaculaceae were observed in SFQSeM group.

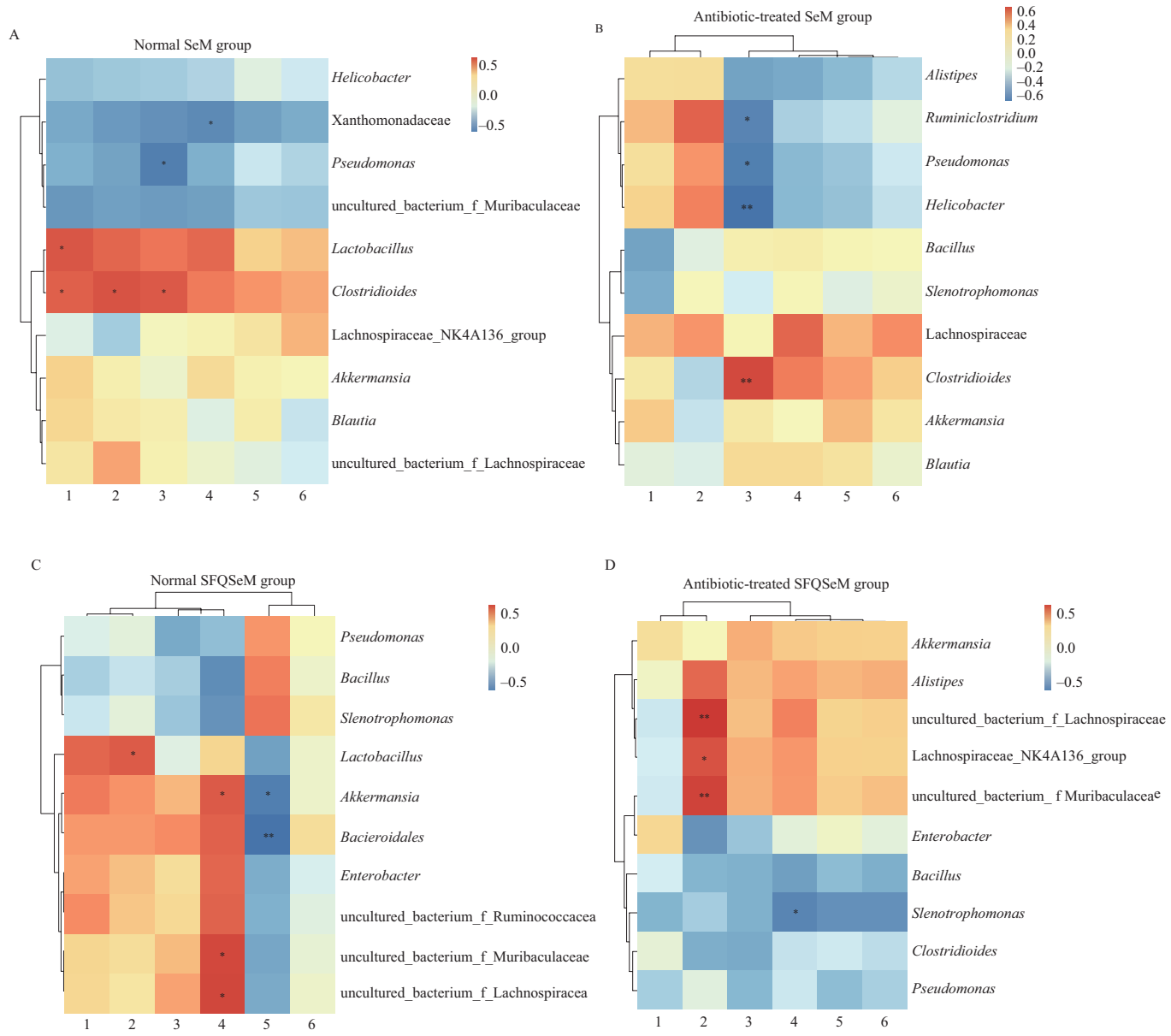

Fig. 9 Associations between intestinal microbiota and selenium relative indexes in serum and liver. (A) normal SeM group. (B) antibiotic-treated SeM group group. (C) normal SFQSeM group, and (D) antibiotic-treated SFQSeM group. 1: selenium concentration in mice serum. 2: GSH-Px activity in mice liver. 3: GSH-Px activity in mice serum. 4: *GPx-1* mRNA level in mice liver. 5: *TXNRD1* mRNA level in mice liver. 6: *Sepp1* mRNA level in mice liver. Data is analysed using Pearson's correlation analyses and presented as correlation coefficients (*r*). * indicates the correlation is significant at the 0.05 level.

4. Discussion

4.1 The influence of the intestinal microbiota on the antioxidant activity of SFQSeM in vivo

Growing evidence suggests that the redox status of the host is closely linked to the intestinal microbiota[23]. Excessive ROS produced under oxidative stress can disrupt intestinal microbiota and metabolic homeostasis by impairing mitochondrial function[24]. Sustained oxidative stress alters the intestinal hypoxic environment, promoting the proliferation of opportunistic anaerobes and causing dysbiosis, which further disrupts the intestinal microbiota structure[25]. *Lactobacillus* plays a crucial role in human health, particularly in maintaining the balance of the microbiome in various body systems[26]. It alleviates oxidative damage by producing antioxidant metabolites (such as lactic acid, acetic acid, exopolysaccharides, carotenoids, and ferulic acid), and enhancing host antioxidant enzyme activities, such as SOD and GSH-Px[26-27]. Similarly, Lachnospiraceae_NK4A136_group, a butyrate-producing bacterial strain, has anti-inflammatory properties and regulates autophagy in colonic epithelial cells[28-29]. In this study, the reduced antioxidant effects of SFQSeM observed in antibiotic-treated mice suggest that the microbiota is essential for promoting its efficacy. Importantly, antioxidant selenium markers and antioxidant parameters were positively associated with *Lactobacillus*. *Lachnobacterium*, Muribaculaceae, and Lachnospiraceae_NK4A136_group also had a positive correlation with the selenium markers. These findings highlight the critical role of these specific intestinal bacteria in modulating the antioxidant properties of selenium-containing peptides. Increased levels of lactate and butyrate were observed in both SFQSeM-intervened *D*-gal-treated mice and antibiotic-treated mice, which

provided the basis for elevated antioxidant levels in mice[29].

The peptide sequence has also been reported to facilitate interaction with intestinal microbiota, which convert peptides into bioactive forms[30]. Research suggests that bioactive peptides modulatethe gut environment, resulting in changes in the gut microbiome and metabolites. These changes may act as signalling molecules to activate the antioxidant pathway[31]. For example, selenium-free soy peptides also serve as intestinal microbiota modulators, altering the composition of the microbiota and the metabolites released[32]. In particular, glutamine (Gln) serves as an energy source for intestinal epithelial cells and lymphocytes, as well as producing other genetic material useful to intestinal bacteria. Dietary supplementation of Gln may have beneficial effects in reducing the symptoms of inflammatory disorders and may protect the intestinal against the damaging effects of oxidative stress[33]. Therefore, we suggest that the selenium-peptide sequence interplay enhances the overall bioactivity of SFQSeM, distinguishing it from simpler selenium compounds such as SeM, which lack this sequence-specific interaction.

4.2 Intestinal microbiota contribution to SFQSeM bioavailability

The intestine is a key site for the absorption and metabolism of bioactive peptides. Peptides are degraded in the gastrointestinal tract into smaller peptides and amino acids, and absorbed by intestinal cells[34]. However, some undigested peptides may escape absorption and interact with the gut microbiota, where they can be further metabolised. Thus, the microbiota plays a critical role in regulating the bioavailability and biological activity of dietary compounds[35]. Although SFQSeM remains stable during *in vitro* gastrointestinal digestion, its absorption efficiency is limited. Our previous study showed that SFQSeM is transported across Caco-2 monolayers via the paracellular pathway, but with a low transport rate of only 8.63%, which is significantly lower than that of SeM[15]. This reduced absorption efficiency may limit the direct bioavailability of SFQSeM, thereby increasing its potential for interaction with the intestinal microbiota.

Previous studies have shown that germ-free mice had higher serum and liver selenium concentrations and increased hepatic *GPx-1* expression, as well as GSH-Px and TXNRD activities after SeM supplementation compared to normal mice[36]. Similarly, Takahashi et al.[37] found that selenium compounds such as SeM and SeC significantly increased serum GPx-3 and Sepp1 levels in antibiotic-treated mice. These findings suggest a competitive interaction between the host and microbiota for selenium absorption, which may limit selenium availability to the host and reduce the efficacy of selenium-dependent proteins in critical organs like the liver. In our study, SeM supplementation resulted in higher hepatic GSH-Px activity and *GPx-1* expression in antibiotic-treated mice compared to the control group. However, after SFQSeM supplementation, these selenium markers were significantly lower in the antibiotic-treated group than in the normal group. As previously discussed, selenium-containing peptides like SFQSeM may not be fully absorbed in the small intestine but instead interact with the gut microbiota, which metabolizes them into bioactive compounds that contribute to antioxidant activity[32]. Consistent with this notion, the bioavailability of 1β-methylseleno-*N*-acetyl-*D*-galactosamine (SeSug1) is significantly reduced in antibiotic-suppressed rats, further highlighting the role of the microbiota in determining selenium availability[37-38]. Furthermore, our results suggest that *Bacteroides*, a prominent genus of protein metabolising bacteria in the gut[39-40], is a characteristic microbiota associated with SFQSeM administration (Fig. 7B). Compared to the saline, Na_2SeO_3 and SeM groups, SFQSeM supplementation significantly improved pathways related to amino acid synthesis, metabolic processes and secondary metabolite production (Figs. 8E, F). These findings highlight the microbiota's pivotal role in modulating the bioavailability and antioxidant activity of SFQSeM, providing further evidence for its functional dependence on microbial metabolism.

5. Conclusion

This study demonstrates that the antioxidant activity of the tetrapeptide SFQSeM is closely associated with its ability to modulate the intestinal microbiota. SFQSeM supplementation significantly enhanced antioxidant status in mice, improving hepatic GSH-Px activity, *GPx-1* expression, and beneficial shifts in intestinal microbial composition and metabolites in both *D*-gal-treated and antibiotic-treated mouse models. Key probiotic strains such as *Lactobacillus*, Lachnospiraceae NK4A136 group, and Muribaculaceae were strongly correlated with hepatic selenium antioxidant markers, highlighting the crucial role of the intestinal microbiota in mediating SFQSeM's antioxidant effects *in vivo*. Future research will focus on elucidating the structural properties of SFQSeM that facilitate its microbiota-modulating effects, and the identification of key metabolites contributing to its systemic antioxidant benefits.

Conflict of interest

Chenyang Lu is an editorial board member for *Food Science and Human Wellness* and was not involved in the editorial review or the decision to publish this article. The authors confirm that they have no conflicts of interest with respect to the work described in this manuscript.

Acknowledgments

Financial support from the National Natural Science Foundation of China (32502106), One health Interdisciplinary Research Project, Institute of One Health Science, Ningbo University (NBUOH202502) and the Ningbo Top Talent Project (215-432094250) . The support of the Key Laboratory of the Institute of New Drug Technology, Ningbo University is gratefully acknowledged.

Appendix A. Supplementary data

Supplementary data associated with this article can be found, in the online version, at http://doi.org/10.26599/FSHW.2025.9250494.

References

[1] R. Vona, L. Pallotta, M. Cappelletti, et al., The impact of oxidative stress in human pathology: focus on gastrointestinal disorders, Antioxidants 10 (2021) 201. https://doi.org/10.3390/antiox10020201.

[2] M. Başeğmez. An overview of the antioxidant and anti-inflammatory activity of selenium. IntechOpen: London, 2023.
[3] S.K. Walsh, K. Pettigrew, I. Mezzani, et al., Role of selenium and 17β oestradiol in modulating lipid accumulation in *in vitro* models of obesity and NAFLD, Food & Medicine Homology 2 (2025) 9420056. https://doi.org/10.26599/FMH.2025.9420056.
[4] G. Bjørklund, M. Shanaida, R. Lysiuk, et al., Selenium: an antioxidant with a critical role in anti-aging, Molecules 27 (2022) 6613. https://doi.org/10.3390/molecules27196613.
[5] J. Chaudière, Biological and catalytic properties of selenoproteins, Int. J. Mol. Sci. 24 (2023) 10109. https://doi.org/10.3390/ijms241210109.
[6] Y. Sun, Z. Wang, P. Gong, et al., Review on the health-promoting effect of adequate selenium status, Front. Nutr. 10 (2023) 1136458. https://doi.org/10.3389/fnut.2023.1136458.
[7] Y. Xiong, Y. Huang, L. Li, et al., A review of plant selenium-enriched proteins/peptides: extraction, detection, bioavailability, and effects of processing, Molecules 28 (2023) 1223. https://doi.org/10.3390/molecules28031223.
[8] K. Liu, R. Du, F. Chen, Stability of the antioxidant peptide SeMet-Pro-Ser identified from selenized brown rice protein hydrolysates, Food Chem. 319 (2020) 126540. https://doi.org/10.1016/j.foodchem.2020.126540.
[9] S. Wu, Z. Zhu, M. Chen, et al., Comparison of neuroprotection and regulating properties on gut microbiota between selenopeptide Val-Pro-Arg-Lys-Leu-SeMet and its native peptide Val-Pro-Arg-Lys-Leu-Met *in vitro* and *in vivo*, J. Agri. Food Chem. 71 (2023) 12203-12215. https://doi.org/10.1021/acs.jafc.3c02918.
[10] J. Cai, W. Su, X. Chen, et al., Advances in the study of selenium and human intestinal bacteria, Front. Nutr. 9 (2022) 1059358. https://doi.org/10.3389/fnut.2022.1059358.
[11] S. Ramírez-Acosta, M. Selma-Royo, M.C. Collado, et al., Selenium supplementation influences mice testicular selenoproteins driven by gut microbiota, Sci. Rep. 12 (2022) 4218. https://doi.org/10.1038/s41598-022-08121-3.
[12] R.L.U. Ferreira, K.C.M. Sena-Evangelista, E.P. De Azevedo, et al., Selenium in human health and gut microflora: bioavailability of selenocompounds and relationship with diseases, Front. Nutr. 8 (2021) 685317. https://doi.org/10.3389/fnut.2021.685317.
[13] A.M. Pereira, C. Pinna, G. Biagi, et al., Supplemental selenium source on gut health: insights on fecal microbiome and fermentation products of growing puppies, FEMS Microbiol. Ecol. 96 (2020) fiaa212. https://doi.org/10.1093/femsec/fiaa212.
[14] X. Zhang, L. Jia, H. He, et al., Modulation of oxidative stress and gut microbiota by selenium-containing peptides from enshiensis *Cardamine enshiensis* and structural-based characterization, Food Chem. 395 (2022) 133547. https://doi.org/10.1016/j.foodchem.2022.133547.
[15] X. Zhang, H. He, J. Xiang, et al., Screening and bioavailability evaluation of anti-oxidative selenium-containing peptides from soybeans based on specific structures, Food Funct. 13 (2022) 5252-5261. https://doi.org/10.1039/D2FO00113F.
[16] H. Han, Z. Liu, J. Yin, et al., *D*-Galactose induces chronic oxidative stress and alters gut microbiota in weaned piglets, Front. Physiol. 12 (2021) 634283. https://doi.org/10.3389/fphys.2021.634283.
[17] D.R. Goulding, P.H. Myers, A.B. Dickerson, et al., Comparative efficacy of two types of antibiotic mixtures in gut flora depletion in female C57BL/6 mice, Comp. Med. 71 (2021) 203-209. https://doi.org/10.30802/AALAS-CM-21-000023.
[18] J. Zhao, F. Tian, N. Zhao, et al., Effects of probiotics on d-galactose-induced oxidative stress in plasma: a meta-analysis of animal models, J. Function. Foods 39 (2017) 44-49. https://doi.org/10.1016/j.jff.2017.09.055.
[19] M.S. Alam, J. Gangiredla, N.A. Hasan, et al., Aging-induced dysbiosis of gut microbiota as a risk factor for increased *Listeria monocytogenes* infection, Front. Immunol. 12 (2021) 672353. https://doi.org/10.3389/fimmu.2021.672353.
[20] W.L. George, *In vitro* antibacterial activity of the combination of clindamycin and ceftazidime, Antimicrob. Agents Chemother. 25 (1984) 657-658. https://doi.org/10.1128/aac.25.5.657.
[21] P. Acred, D. Brown, D. Turner, et al., Pharmacology and chemotherapy of ampicillin—a new broad-spectrum penicillin, Br. J. Pharmacol. 18 (1962) 356-369. https://doi.org/10.1111/j.1476-5381.1962.tb01416.x.
[22] C. Thiry, A. Ruttens, L. De Temmerman, et al., Current knowledge in species-related bioavailability of selenium in food, Food Chem. 130 (2012) 767-784. https://doi.org/10.1016/j.foodchem.2011.07.102.
[23] B. Yun, M. King, M.S. Draz, et al., Oxidative reactivity across kingdoms in the gut: host immunity, stressed microbiota and oxidized foods, Free Radical Biol. Med. 178 (2022) 97-110. https://doi.org/10.1016/j.freeradbiomed.2021.11.009.
[24] J.W.O. Ballard, S.G. Towarnicki, Mitochondria, the gut microbiome and ROS, Cell. Signal. 75 (2020) 109737. https://doi.org/10.1016/j.cellsig.2020.109737.
[25] J. Apajalahti, K. Vienola, Interaction between chicken intestinal microbiota and protein digestion, Anim. Feed Sci. Technol. 221 (2016) 323-330. https://doi.org/10.1016/j.anifeedsci.2016.05.004.
[26] T. Feng, J. Wang, Oxidative stress tolerance and antioxidant capacity of lactic acid bacteria as probiotic: a systematic review, Gut Microbes 12 (2020) 1801944. https://doi.org/10.1080/19490976.2020.1801944.
[27] Y.F. Liu, N. Ling, B. Zhang, et al., Flavonoid-Rich mulberry leaf extract modulate lipid metabolism, antioxidant capacity, and gut microbiota in high-fat diet-induced obesity: potential roles of FGF21 and SOCS2, Food & Medicine Homology 1 (2024) 9420016. https://doi.org/10.26599/FMH.2024.9420016.
[28] H.M. Abdel-Latif, M. Abdel-Tawwab, M.A. Dawood, et al., Benefits of dietary butyric acid, sodium butyrate, and their protected forms in aquafeeds: a review, Rev. Fish. Sci. Aquacult. 28 (2020) 421-448. https://doi.org/10.1080/23308249.2020.1758899.
[29] S. Zhang, D. Feng, J. An, et al., Total Glycosides of Cistanche deserticola attenuates DSS-induced inflammatory bowel disease by regulating intestinal environmental homeostasis, Food & Medicine Homology 2 (2025) 9420048. https://doi.org/10.26599/FMH.2025.9420048.
[30] Z. Chu, L. Zhu, Y. Zhou, et al., Targeting Nrf2 by bioactive peptides alleviate inflammation: expanding the role of gut microbiota and metabolites, Crit. Rev. Food Sci. Nutr. 65 (2025) 3314-3333. https://doi.org/10.1080/10408398.2024.2367570.
[31] I.U. Okagu, J.C. Ndefo, E.C. Aham, et al., Lupin-derived bioactive peptides: intestinal transport, bioavailability and health benefits, Nutrients 13 (2021) 3266. https://doi.org/10.3390/nu13093266.
[32] T.J. Ashaolu, Soy bioactive peptides and the gut microbiota modulation, Appl. Microbiol. Biotechnol. 104 (2020) 9009-9017. https://doi.org/10.1007/s00253-020-10799-2.
[33] Y. Ma, X. Han, J. Fang, et al., Role of dietary amino acids and microbial metabolites in the regulation of pig intestinal health, Anim. Nutr. 9 (2022) 1-6. https://doi.org/10.1016/j.aninu.2021.10.004.
[34] Z. Yan, Y. Gui, C. Liu, et al., Gastrointestinal digestion of food proteins: anticancer, antihypertensive, anti-obesity, and immunomodulatory mechanisms of the derived peptides, Food Res. Int. 189 (2024) 114573. https://doi.org/j.foodres.2024.114573.
[35] Z. Yang, S.F. Liao, Physiological effects of dietary amino acids on gut health and functions of swine, Front. Vet. Sci. 6 (2019) 169. https://doi.org/10.3389/fvets.2019.00169.
[36] J. Hrdina, A. Banning, A. Kipp, et al., The gastrointestinal microbiota affects the selenium status and selenoprotein expression in mice, J. Nutr. Biochem. 20 (2009) 638-648. https://doi.org/10.1016/j.jnutbio.2008.06.009.
[37] K. Takahashi, N. Suzuki, Y. Ogra, Effect of gut microflora on nutritional availability of selenium, Food Chem. 319 (2020) 126537. https://doi.org/10.1016/j.foodchem.2020.126537.
[38] K. Takahashi, N. Suzuki, Y. Ogra, Bioavailability comparison of nine bioselenocompounds *in vitro* and *in vivo*, Internatio. J. Molecular Sci. 18 (2017) 506. https://doi.org/10.3390/ijms18030506.
[39] H. Huang, H.B. Krishnan, Q. Pham, et al., Soy and gut microbiota: interaction and implication for human health, J. Agric. Food Chem. 64 (2016) 8695-8709. https://doi.org/10.1021/acs.jafc.6b03725.
[40] V.T. Rist, E. Weiss, N. Sauer, et al., Effect of dietary protein supply originating from soybean meal or casein on the intestinal microbiota of piglets, Anaerobe 25 (2014) 72-79. https://doi.org/10.1016/j.anaerobe.2013.10.003.